Journal of Applied Polymer Science

Antimicrobial carbon materials incorporating copper nano-crystallites and their PLA composites

Anna Ilnicka,[1] Mariusz Walczyk,[1] Jerzy P. Lukaszewicz,[1] Katarzyna Janczak,[2] Rafal Malinowski[2]
[1]Faculty of Chemistry, Nicolaus Copernicus University, Faculty of Chemistry, 7 Gagarina Street, Torun 87-100, Poland
[2]Institute for Engineering of Polymer Materials and Dyes, 55 M. Sklodowskiej-Curie Street, Torun 87-100, Poland
Correspondence to: A. Ilnicka (E-mail: annakucinska@o2.pl)

ABSTRACT: In the first stage, carbon materials were manufactured from chitin and chitosan as the main precursor. Chitin and chitosan were impregnated with Cu^{2+} ions. Using heat treatment, the organic matter (biopolymers) was transformed into a porous carbon matrix, while copper ions were transformed into copper-based nano-crystallites containing copper atoms in a +1 and 0 oxidation state. Such synthesized carbons exhibited high contact antifungal activity, e.g., for sample, CH-ACu0.1_Ox against *R. nigricans* the inhibition zone is 10.27 mm. In the second stage, composite polymer films were manufactured by mixing polylactide (PLA) and the obtained microbial carbon material (up to 3 wt % Cu-carbon content). Despite the very low content of carbon material (3 wt %), the composite PLA films exhibited excellent microbial properties for selected bacteria and fungi, e.g., sample CuCM3%/PLA demonstrated high $\log_{10}$ reduction values of 2.17 and 2.66 for the strains of *E. coli* and *S. aureus*, respectively. The composite films, and their components, were examined by means of diversified physicochemical methods like low temperature adsorption of nitrogen, SEM, elemental analysis, XRD, cyclic voltammetry, antifungal, and antibacterial analysis. © 2016 Wiley Periodicals, Inc. J. Appl. Polym. Sci. **2016**, *133*, 43429.

KEYWORDS: biodegradable; composites; manufacturing; mechanical properties; properties and characterization

Received 6 September 2015; accepted 7 January 2016
DOI: 10.1002/app.43429

INTRODUCTION

Most publications on the microbial properties of carbon materials relate to the presence of silver nanoparticles, e.g., activated carbon fibres supporting silver exhibited strong lethal activity against *Escherichia coli*, *Saccharomyces cerevisiae*, and *Pichia pastoris*. The microbicidal property of activated carbon is also very important in order to decrease the risk of water and air contamination with microorganisms like *E. coli*.[1–3] Silver ions have been widely used as disinfectants that inhibit bacterial growth by disrupting some essential enzymatic functions of the microorganism via interaction with the thiol-group.[4] Copper and silver bimetal-dispersed polymeric beads were also investigated, exhibiting significantly larger antibacterial activities than single metal-doped (Cu or Ag) beads, for both gram-positive *Staphylococcus aureus* and gram-negative *E. coli* bacteria. The prepared bimetal beads remained effective, completely inhibiting the bacterial growth, which makes them potential antibacterial agents for water purification.[5]

The first evidence that copper fungicides kill scab spores by inhibiting mitochondrial respiration indicated that the antifungal action of the slightly and insoluble copper hydroxide and copper oxide, respectively, cannot be explained based on the concentration of dissolved copper ions.[6] The use of antibacterial and antifungal active silica submicrospheres with metallic silver and copper nano-precipitates in textile-polymeric coating materials has been presented, too.[7]

The antifungal activity was achieved against numerous plant pathogens and mycotoxin producing moulds at relatively low concentration of the agents.[8] Besides that, new copper-containing fungicides were developed based on granulated peat and powder-like anthracite as supports.[9] Cubic and octahedral Cu_2O microcrystals were synthesized by the reduction of copper–ligand complexes with glucose under microwave irradiation. The Cu_2O microcrystals were tested for antibacterial activity against *E. coli*. The antibacterial activity of the cubic Cu_2O crystals was superior to that of the octahedral Cu_2O crystals.[10]

Other microbial materials containing copper, e.g., regenerated cellulose films coated with copper nanoparticles, were prepared from a cellulose cuprammonium solution through coagulation. The films coated with Cu nanoparticles showed efficient antibacterial activity against *S. aureus* and *E. coli*.[11] Polypropylene composites containing different amounts of copper nanoparticles were tested as a microbial material, too. The composites were prepared by the "melt mixed" method and drastically reduced the life-time of bacteria.[12] According to our knowledge,

microbial activity of activated carbon supported Cu derivatives have not been tested yet.

The purpose of the present work is to elaborate a synthesis method of novel Cu-activated carbon microbial materials, as well as to investigate their antifungal and antibacterial activity. Particular attention will be paid to the ease of manufacturing and a low production costs. The second aim is to incorporate such carbons in biodegradable polymeric films, aiming at the fabrication of composite packing foils showing antibacterial activity. The general aim will be achieved in several steps, like: (i) preparation of new copper-containing carbon materials; (ii) study of the structural and microbial properties of obtained carbons; (iii) obtaining of new microbial films; (iv) study of the properties of the obtained films.

EXPERIMENTAL

Preparation of Copper-Loaded Carbon Materials (CuCMs)

Chitin (CA), or chitosan (CH), in the amount of 5 g was treated with an aqueous solution of $Cu(NO_3)_2$ (ACu) at a concentration ranging from 0.05 to 0.1*M* (0.05, 0.1), with a volume of 50 cm^3. Copper loading lasted for 24 h at room temperature. Dry chitin (chitin from shrimp shells, CAS Number: 1398-61-4) and chitosan powder (physical form >75% deacetylation, medium molecular weight, CAS Number: 9012-76-4) were provided by Sigma Aldrich. During the synthesis, Cu^{2+} ions coordinately bound to primary amine (chitosan), secondary amine (chitin), or hydroxyl groups (chitin, chitosan). The resulting mass was allowed to drain off excess water. The whole was then transferred to a tube furnace, wherein the mass was kept in the flow of nitrogen with an oxygen content of 0.1% by volume. The tube furnace was equipped with a vent. The inert gas flowed through a hole, carrying the gaseous carbonization products of chitin or chitosan. The tube furnace was heated gradually, at the heating rate of 10 °C/min, to 700 °C. Once the set temperature was achieved, the obtained carbon material was soaked for 1 h.

Instrumental Analysis of CuCMs

Specific Surface Area Measurements. The structural parameters of the carbon materials were characterized by low-temperature nitrogen adsorption. The relevant isotherms of all the samples were measured at 77 K on an ASAP 2010 volumetric adsorption analyser (Micromeritics, USA). Before each adsorption measurement, the sample was outgassed under vacuum at 200 °C.

Scanning Electron Microscopy. The carbons were examined by scanning electron microscopy (SEM, 1430 VP, LEO Electron Microscopy) with energy dispersive X-ray spectrometer (EDX, Quantax 200; detector: XFlash 4010, Bruker AXS).

X-Ray Powder Diffraction Analysis. X-ray diffraction (XRD) spectra were measured by means of a CuKα source in the range of 2Θ from 10° to 90° (X-Pert PRO Systems, Philips).

Elemental Analysis

The carbon materials were analysed (Vario MACRO CHN, ELEMENTAR Analysensysteme GmbH) for their total carbon and nitrogen contents.

Cyclic Voltammetry Analysis and Electrochemical Oxidation

Cyclic voltamperometry curves (CV) were recorded using a computer-controlled Autolab (Eco Chemie) modular electrochemical system, equipped with a PGSTAT128N potentiostat, controlled by the NOVA software. The measurements were carried out using a three-electrode electrochemical cell presented in one of our earlier papers.[13–18] The working electrode, in this system, was an about 3 mm thick sedimentation layer of powder carbon material on a platinum plate, which served as an electrical contact. The counter electrode was a platinum wire, and a silver chloride electrode was a reference electrode (Ag/AgCl in 3*M* KCl). After vacuum desorption (10^{-2} Pa), the carbon sample (mass = 200 mg) was placed in an electrode container and drenched with a deaerated solution (1*M* KCl; usually after 24 h) to obtain a ~3 mm sedimentation layer on the Pt contact plate. The potentiometric responses of the carbon electrodes were measured in oxygen-free electrolyte solutions. Cyclic voltammetric curves (CVs) were recorded for 5 mV s^{-1} and 10 mV s^{-1} sweep amplitudes once the electrochemical equilibrium had been established (no changes in repeated CV scans). The starting material, after recording the voltammograms, was oxidized (Ox) in the same electrochemical cell, the applied voltage was 1.5 V, in relation to Ag/AgCl in 3*M* KCl over 1200 s. After the oxidation process, cyclic voltamperometry curves (CV) were recorded (sweep rate 5 and 10 mV s^{-1}). The anodized carbon material was then filtered, washed, and subjected to drying at 100 °C for several hours. All measurements and oxidation were carried out in a thermostated system at room temperature (293 K).

Antibacterial Activity of CuCMs and Films

Antibacterial properties of powdered carbon materials were examined with a special procedure. The liquid culture of microorganism was conducted in saline solution (0.85% NaCl in distilled water). Two model strains of bacteria were used: *E. coli* (ATCC 8739) and *S. aureus* (ATCC 6538 P). The study was conducted in sterile 50 mL Erlenmeyer flasks containing 20 mL of the saline solution. This solution was inoculated with individual strains of bacteria, leading to the turbidity of solutions equal to 0.5 McFarland standard (McF). After inoculation, 0.01 g of carbon material was added to each Erlenmeyer flask. The control was a suspension of microorganisms in NaCl without carbon material. All Erlenmeyer flasks were incubated with shaking for 24 h at 35 °C. After incubation, the microorganisms were recovered by serial dilution. With the dilution from 10^{-1} to 10^{-6}, 1-mL suspensions were transferred into sterile Petri dishes (diameter 90 mm) and overflowed with 25 mL of plate count agar (PCA) media (OXOID) at 45 °C. Petri dishes were incubated for 48 h at 35 °C. After this time, the bacterial colony forming units (CFU) were counted. The results were presented as the difference between the logarithm of the average number of CFU in control samples, and the logarithm of the average CFU number in test samples. The experiment was repeated three times.

Antibacterial properties of PLA films, containing the active substance about 0.1, 0.5, 1.0, and 2.0 wt % concentration, were indicated. The control of PLA films did not contain the active substance. The test was carried out according to the ISO22196:2011 standard (Measurement of antibacterial activity on plastic and other nonporous surfaces). The same reference strains of bacteria were applied as when testing the powder materials. The size, the shape of the sample, materials, the

methodology of examinations and guidelines were described in the applied standard.

Antifungal Activity of CuCMs

The antifungal activity of copper carbon materials was tested. The laboratory equipment was sterilized by thermal (2 h, 160 °C) and chemical (ethanol 70%, Meliseptol) methods. Microfungi (*R. nigricans*) were cultured on a solid carbohydrate microbiological substrate (pepton K/agar-agar/glucose) during incubation at 20–22 °C. The powdered samples of CuCMs were placed in the middle of the microbiological substrate to ensure contact with growing moulds. Inoculation was performed by spraying spores of mould over the test sample. After 5 days incubation, the diameter of inhibition zone was measured using the calliper in triplicate. The measure values were denoted in millimetres (mm).

Preparation of CuCM/PLA Composites

Polylactide (PLA) and copper carbon material (described in 2.1) were used for the preparation of new composites. The polymer used in this study was PLA (type 2003D, Nature Works, USA) in the form of granules having an average molecular weight of 79,000 Da and containing 3.5% of units (*D*), and 96.5% of units (*L*). The mixture was prepared from two components: PLA in a weight ratio from 97 to 99.9 wt % (dried for 4 h at 60–80 °C, in order to remove moisture before processing) and carbon material in a weight ratio from 0.1 to 3 wt %, respectively. The components were processed in a co-rotating twin-screw extruder (BTSK 20/40D, Bűhler, Germany). The extruder was equipped with screws having a diameter (*D*) of 20 mm, a length (*L*/*D*) of 40, and the ability to change shape. The extrusion process was performed without free degassing and without pressure degassing at a constant screw speed of 250 min^{-1}. The following temperatures of cylinder zone of a co-rotating twin screw extruder were set: 175, 180, 185, and 190 °C.

During extrusion, screws of special shape were used to provide a proper dispersion and distribution of the dispersed phase in the matrix of the PLA. The extrusion was performed using PLA as a polymer matrix and consisted of two stages: Stage I—extrusion of concentrate-containing carbon filler; Stage II—dilution of the concentrate produced in the first stage to the appropriate concentrations. The two-step process was developed in order to allow for the best possible distribution and dispersion of the dispersed phase in the polymer matrix. As a result, five composites were extruded, as well as a reference sample (pure PLA).

The produced granulate was applied for manufacturing of standardized test bars, shaped using a laboratory injection moulding press, type PLUS 35/75 (Battenfeld, Germany).

Extrusion of the composite films was performed at the following temperatures of particular cylinder zones of the single screw extruder Plasti Corder PLV151 (Brabender, Germany): 180, 190, and 190 °C. The temperature of the extrusion die head was 180 °C, and the screw rotational speed was 30 min^{-1} (constant). The temperature of the rollers was 50 °C.

Rheological, Mechanical, and Optical Analysis of CuCM/PLA Composites

The melt flow rate and impact strength tests were analysed for properties of the composite. The transmittance and haze measurements were made on the film produced from the composite.

Melt Flow Rate (MFR)

The MFR was measured by using a capillary plastometer (type LMI 4003, Dynisco, Germany) at 190 °C under a piston loading of 2.16 kg. Determination of the MFR was carried out according to a relevant standard: PN-EN ISO 1133:2005.

Haze and Transmittance

The Spherical Hazemeter (Diffusion Systems, UK) was utilized to investigate transmittance and haze for the films of composite samples. Transmittance and haze tests were executed according to PN-EN ISO 13468-1.

Mechanical Properties

All composites CuCM/PLA were tested and compared in terms of their mechanical properties.

A tensile testing machine, type TIRAtest 27025 (TIRA Maschinenbau GmbH, Germany), designed to examine mechanical properties under static tension was used. Tensile strength, tensile stress at break and elongation at break of elasticity were evaluated according to the PN-EN ISO 527-1:1998 standard, using the extension rate of 10.0 mm/min.

Impact strength was evaluated with a Pendulum Impact Tester, type IMPats-15 (ATS FAAR, Italy), intended for determination of Charpy impact strength, according to the PN-EN ISO 179-1:2010 standard.

RESULTS AND DISCUSSION

Morphology, Surface Area, and Elemental Composition

Before fabrication of microbial foils, Cu-incorporating carbons, denoted as CuCMs, were subjected to multidirectional characterization. The results were essential for the optimization of the fabrication of microbial foils.

Specific surface area (S_{BET}) and elemental content of manufactured samples (before and after oxidation) are shown in Table I. The S_{BET} of the CuCMs, obtained from chitin, were generally larger for CA-ACu0.05 and CA-ACu0.1 samples than for chitosan-originated ones. The performed oxidation led to samples of reduced surface area in general. The rate of reduction was sometimes very spectacular, like some chitosan-originated CuCMs (CH-ACu0.05_Ox and CH-ACu0.1_Ox). The results proved some previous observations that carbonization of virgin chitosan yields a nonporous carbon matrix of extremely low surface area (CH and CH_Ox samples) while carbonization of chitin instantly yield a porous carbon matrix of high surface area (CA and CA_Ox samples). As mentioned, oxidation of the samples reduced their surface area. This effect can be attributed to the oxidative dissolution of the most exposed and reactive parts of the carbon matrix. The reactive centres usually exist in pores and cavities, of which occurrence determines a specific surface area. Thus, intensive oxidation of porous carbon matrixes results in the vanishing of pore walls and the reduction of pore volume, and surface area.

Table I. BET Surface Area and Elemental Composition (C, H, N, and Other) of Different Samples

Sample	S_{BET} (m^2 g^{-1})	Elemental content (wt %)			
		N	C	H	Other
CA	360	5.7	87.9	1.3	5.1
CA-ACu0.05	455	5.1	74.3	1.5	19.1
CA-ACu0.1	303	5.0	64.6	1.4	29
CH	3	6.9	83.1	1.1	8.9
CH-ACu0.05	123	7.8	70.7	1.5	20
CH-ACu0.1	102	7.9	66.7	1.3	24.1
After oxidation					
CA_Ox	257	6.2	74.6	1.5	17.7
CA-ACu0.05_Ox	359	4.9	71.6	1.6	21.9
CA-ACu0.1_Ox	318	5.0	62.3	1.4	31.3
CH_Ox	8	8.5	75.4	1.5	14.6
CH-ACu0.05_Ox	6	7.0	61.5	1.5	30
CH-ACu0.1_Ox	69	7.0	60.7	1.5	30.8

As presented in Table I, a high nitrogen content, in the range 5.0–8.5 wt %, was observed for all samples. These values are very typical for most of activated carbons obtained from chitin or chitosan. Analogous data were previously reported in some papers.[19–23] Nitrogen atoms play a crucial role in the coordinative bonding of transition metal ions, including copper ions. Uniform distribution of nitrogen atoms in chitin and chitosan enable a uniform distribution of copper ions in the polymers, but also in CuCMs obtained by carbonization of them.

The effect of the precursor type (chitin or chitosan) and concentration of $Cu(NO_3)_2$ on the morphology of CuCMs was investigated. Figure 1 shows some examples SEM images of CuCMs prepared at 700 °C, with different sizes of Cu/Cu_2O (nonoxidized samples) and mainly Cu_2O (particularly of oxidized samples). It can be seen that the materials obtained from chitin [Figure 1(A,B)] contained smaller inorganic crystallites (bright dots) than the carbons obtained from chitosan [Figure 1(C,D)]. The inorganic crystallites were identified as Cu and/or Cu_2O (see further text). The phenomenon can be extended on all investigated samples beside those example ones (Figure 1). Oxidation led to the removal of superficial inorganic crystallites [visible for sample CA-ACu0.05—Figure 1(A)] from the chitin-driven samples [not visible for sample CA-ACu0.05_Ox—Figure 1(B)]. Some crystallites are still present in the subsurface region (gray spots in reduced number).

XRD Results

Figure 2 shows the obtained XRD spectra for CA-ACu0.05 and CH-ACu0.1 samples, before and after oxidation, which are representative for the set of manufactured samples. As shown in Figure 2(A,B), the peaks, which were centred at 43.5 °, 50.6 °, 74,2 °, can be attributed to metallic copper.[24–26] In all of the samples, the peak values, which are located at 36.3 °, 44.2 °, and 77.5 °, correspond to Cu_2O or CuO^*Cu_2O. Furthermore, a peak observed at 38.7 ° is relevant to CuO. Generally, the results mean that more intensities or new peaks of the Cu_2O and CuO^*Cu_2O are observed in the oxidized samples. After oxidation of the CA-ACu0.05 sample and turning it into CA-ACu0.05_Ox sample, all peaks attributed to metallic copper and its derivatives disappeared almost completely [Figure 2(A)]. This effect follows the observed vanishing of superficial copper-based crystallites after oxidation, as demonstrated in Figure 1.

On the contrary, oxidation of chitosan-driven samples did not remove such inorganic crystallites from chitosan-driven specimens like CH-ACu0.1_Ox sample. Still, some sharp peaks are present, but the nature of Cu-based component changed significantly due to oxidation. In the XRD spectrum of non-oxidized sample, CH-ACu0.1 peaks attributed to metallic copper are dominating. After oxidation, the peaks disappear and only peaks attributed to oxidized forms of copper are visible in the spectrum of CH-ACu0.1_Ox [Figure 2(B)]. This effect corresponds to the analysis of morphological changes of chitosan-originated samples [Figure 1(C,D)]. In both cases, i.e., nonoxidized and oxidized chitosan-driven CuCM, inorganic crystallites are intensively grouped on the surface.

In case of chitin-driven nonoxidized sample CA-ACu0.05, copper is present as metallic copper and as oxidized derivatives of copper. It is in contrast to nonoxidized chitosan-driven sample CH-ACu0.1, where metallic copper dominates. Thus, the selection of main precursor for carbon manufacturing, either chitin or chitosan, dramatically influences the chemical state of copper. Oxidation either removes copper (chitin-originated CuCMs) or transforms metallic copper into oxidized derivatives (chitosan-originated CuCMs). This may significantly influence the expected microbial properties of CuCMs and corresponding PLA foils, since the microbial activity is usually ascribed to oxidized form of copper like Cu_2O and/or CuO. The activity is verified experimentally and presented in further sections.

CV Results

Figure 3 depicts CV curves recorded for copper-loaded chitin and chitosan-originated CuCMs using the CA-ACu0.05 and CH-ACu0.1 samples (before and after oxidation), which are representative for the series of manufactured samples. In this figure, there are two redox couples in the potential range from −0.2 to 1.1 V versus Ag/AgCl in 3*M* KCl.

In the series of CV curves [Figure 2(A)] obtained for copper-loaded chitin carbon materials (oxidized and nonoxidized), the profiles are characterized by the presence of only one couple in the measurements potential range. In this case, these peaks with formal potential (E_f) of approximately 0.23 V versus Ag/AgCl in 3*M* KCl, are attributed to the transition $Cu_2O_{(s)}$, $H_3O^+/Cu^0_{(s)}$.

Other samples [Figure 2(B)] are two redox systems exist in the measurements potential range. First redox couple, with formal potential (E_f) of approximately 0.24 V versus Ag/AgCl in 3*M* KCl, correspond to the transition $Cu_2O_{(s)}$, $H_3O^+/Cu^0_{(s)}$. The second redox couple was observed only in the case of chitosan, and is situated in a more positive potential range. It is associated with the reduction and oxidation Cu^{2+}/Cu^+ couple forming a stable complex compound, for example, cyanide, with formal potential of approximately 0.95 V versus Ag/AgCl in 3*M* KCl.

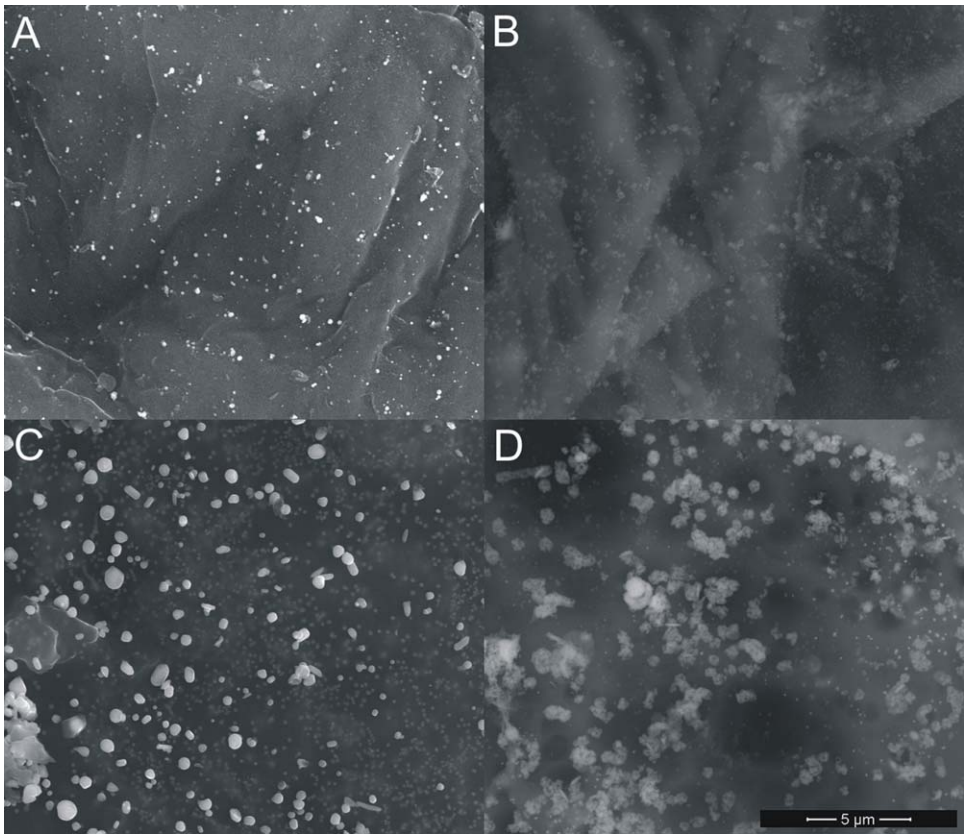

Figure 1. SEM images of carbon materials surface for samples: (A) CA-ACu0.05; (B) CA-ACu0.05_Ox; (C) CH-ACu0.1; (D) CH-ACu0.1_Ox. [Color figure can be viewed in the online issue, which is available at wileyonlinelibrary.com.]

To verify the reversibility of the redox couples, the values of the peak to peak separation (ΔE), the potential at the half height of peaks (E_f), and cathodic to anodic peak ratio as were evaluated diagnostic criteria. The values for the observed redox couple $Cu_2O_{(s)}$, $H_3O^+/Cu^0_{(s)}$ are comparable to the theoretically expected values for a quasi-reversible two-electron process. When chitosan was the CuCM precursor, the electron charge transfer of the peak couple corresponding to the $Cu_2O_{(s)}$, $H_3O^+/Cu^0_{(s)}$ decreased after oxidation. However, an inverse relationship was observed when the precursor of the carbon material was chitin.

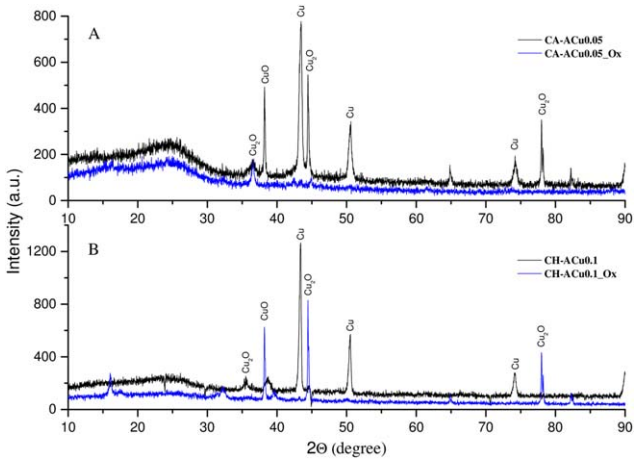

Figure 2. XRD pattern of (A) CA-ACu0.05; CA-ACu0.05_Ox; (B) CH-ACu0.1; CH-ACu0.1_Ox samples. [Color figure can be viewed in the online issue, which is available at wileyonlinelibrary.com.]

Antibacterial Activity of CuCMs on *E. coli* and *S. aureus*

Table II summarizes the results of the microbial activity of powdered carbon materials. The ISO 22196 standard (2011) tells that antibacterial activity can be considered as satisfactory if the value of the $\log_{10}$ reduction in tested samples exceeds 2. Such a material/substance may be called "bactericidal". This criterion was adopted in the current study. According to this condition, nonoxidized chitin-originated CuCMs, i.e., CA-ACu0.05 and

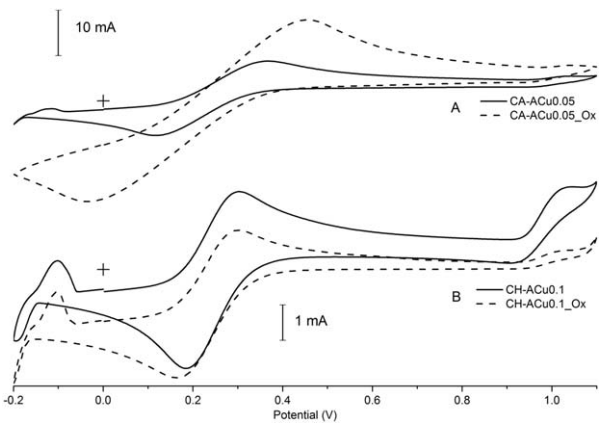

Figure 3. Cyclic voltammogram of powdered carbon electrode materials recorded in 0.1*M* KCl.

Table II. Antibacterial Properties (Reduction of lg_{10} Values) of Powdered Carbons Against *E. coli* and *S. aureus*

Sample	Bacterial strain	Reduction of log10
CA-ACu0.05	*E. coli*	3.55
	S. aureus	1.73
CA-ACu0.1	*E. coli*	1.79
	S. aureus	0.24
CH-ACu0.05	*E. coli*	−0.09
	S. aureus	−0.05
CH-ACu0.1	*E. coli*	2.27
	S. aureus	0.05
After oxidation		
CA-ACu0.05_Ox	*E. coli*	1.63
	S. aureus	0.05
CA-ACu0.1_Ox	*E. coli*	1.08
	S. aureus	−0.1
CH-ACu0.05_Ox	*E. coli*	2.32
	S. aureus	−0.19
CH-ACu0.1_Ox	*E. coli*	2.65
	S. aureus	2.03

CA-ACu0.1 exhibited log_{10} reduction values above 2 or close to this limit for *E. coli* and in part for *S. aureus*. The high bactericidal activity corresponds well to the detected oxidized copper species on the respective surfaces. Oxidation of the chitin-originated CuCMs led to a significant reduction of log_{10} reduction parameter (substantially below 2). The effect can be explained by the removal of copper species after oxidation of chitin-driven CuCMs (proved by SEM and XRD studies). Known literature associates bactericidal properties of copper with the presence of its oxidized forms like Cu_2O and/or CuO.

The last observation can be supported by the data on bactericidal activity of chitosan-originated CuCMs before and after oxidation. Nonoxidized samples CH-ACu0.05 and CH-ACu0.1 exhibited lower bactericidal activity that the ones after oxidation. XRD investigations (Figure 2) proved that oxidation of chitosan-originated CuCMs converted metallic copper into copper oxides to which bactericidal activity is ascribed. Thus, log_{10} reduction values for CH-ACu0.05_Ox and CH-ACu0.1_Ox are in general bigger than for CH-ACu0.05 and CH-ACu0.1 (Table II). Oxidation of chitosan-originated CuCMs is inevitable to trigger bactericidal action of the samples.

Some differences in bactericidal activity occurred regarding the type of bacteria. CH-ACu0.1_Ox sample showed sufficient bactericidal values against both reference strains of *E. coli* and *S. aureus*. The remaining samples demonstrated greater activity against *E. coli* than *S. aureus*, but in the case of CA-ACu0.1, both values were lower than 2. The highest activity, equal to 3.55, was observed for the sample CA-ACu0.05.

Results of Antifungal Properties

The antifungal activity of the manufactured carbons was tested as a function of contact time and the type of CuCMs against *R. nigricans* as shown in Figure 4. All samples inhibited mycelial growth, but the scope and operation differed considerably.

The size of the inhibition zone for samples obtained from chitosan is higher for oxidized samples (as in case of bactericidal tests). The samples of CH-ACu0.05_Ox and CH-ACu0.1_Ox have an inhibition zone of 9.55 and 10.27 mm, respectively. Similar situation is present for sample obtained from chitin, CA-ACu0.05 sample prevent growth of *R. nigricans* microfungi to form an inhibition zone of about 6.82 mm around carbon samples. In the case of the CA-ACu0.05_Ox sample (after oxidation), they have a significantly greater inhibition zone of mycelium growth of 10.02 mm. This effect suggests that (on the contrary to bactericidal test) a contact with carbon matrix contributes to the overall antifungal activity together with an action of copper. For such copper-containing carbon matrixes, a mechanism has been proposed, which exploits simultaneous contact action of carbon matrix and slowly released copper(II) ions, according to the mechanism[13,27]:

$$C<\ldots>C\cdot Cu_2O + H_2O \Longleftrightarrow Cu^{2+} + C<\oplus>C\cdot Cu^0 + 2OH^-$$

$$C<\ldots>N\cdot Cu_2O + H_2O \Longleftrightarrow Cu^{2+} + C<\oplus>N{-}OH\cdot Cu^0 + OH^-$$

where: C<...>C and C<⊕>N is the carbon matrix and carbon matrix with nitrogen moieties, while the <⊕> l is the positive gap in the carbon matrix. Probably, these samples release more Cu^{2+} ions, but with reduced migration in the substrate. During the first and second day of the experiment, a light-blue halo was observed around the CuCM probes, typical for the presence of hydrated Cu(II) ions.

The CA-ACu0.1 and CA-ACu0.1_Ox samples exhibit the narrowest inhibition zone from all samples and have similar values of 5.34 and 5.4 mm, respectively. The carbon materials obtained from chitosan (using 0.1*M* $Cu(NO_3)_2$), have superior antifungal properties relative to the materials obtained from chitin. This phenomenon is due to a difference in the binding of copper ions from CH or CA (the formation of the coordination bond with the $-NH_2$ or $-OH$). As a result, for a given concentration of a compound of copper(II) have reached on carbon various chemical forms of the same chemical compounds responsible for the antifungal properties.

The mechanism of microbial/biostatic involves several phenomena[28–32]:

1. The surface carbon material, through its strong adsorption properties, involves the cell wall of microorganisms;
2. The surface copper(I) oxide and metallic copper slowly release copper(II) ions, exhibiting a high toxicity to the outer membrane of microorganisms. Contact with water leads to the release of ions, which then become absorbed by pathogens;
3. It has been found that a smaller particle size of <2 μm (shown in Figure 1 for samples obtained from chitin) generates more positive charge, which allows for a stronger bond with the negatively charged surface on which the infection occurs, allowing the compound to effectively combat pathogens;
4. Fenton-like copper redox mechanism: oxidative damage generated by reactive oxygen species, such as hydrogen peroxide, hydroxyl radical, superoxide radical anion.

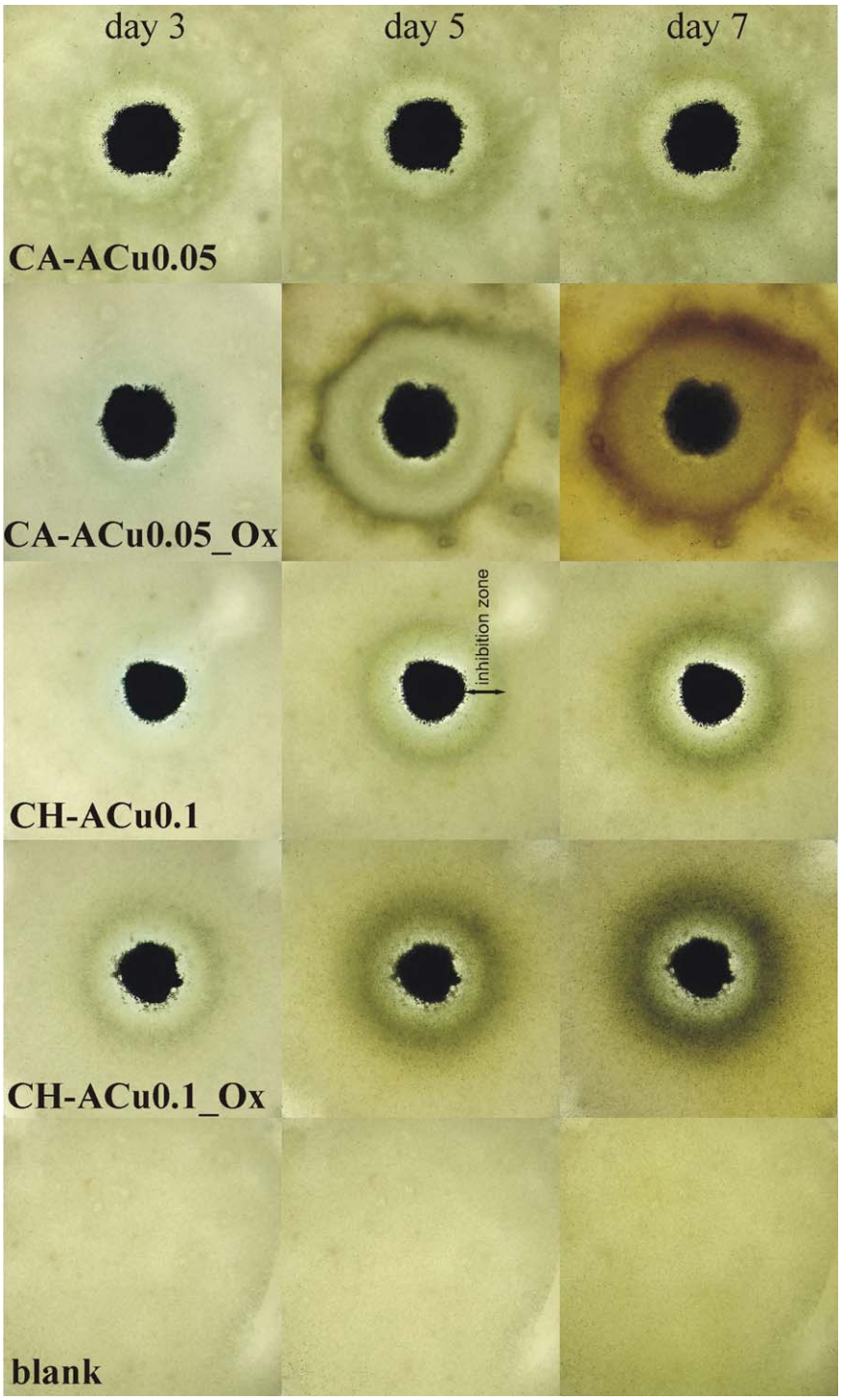

Figure 4. Antifungal activity of different carbon samples as a function of time against *R. nigricans*. [Color figure can be viewed in the online issue, which is available at wileyonlinelibrary.com.]

Rheological, Mechanical, and Optical Results of CuCM/PLA Composites

The contemporary food market creates a high demand for biodegradable packing materials, which additionally exhibit microbial properties. Such packaging should protect human health, the environment, and should be attractive from the economic point of view. Ease of manufacturing plays a crucial role, too. Polylactide (PLA), is one of the most important biodegradable polymers. These plastics are being used not only in medicine (e.g., tissue engineering) and automobile components, but also in the manufacturing of everyday items, e.g., containers, packages, and so on. PLA may exhibit various physicochemical properties that essentially

Table III. Results of Rheological, Mechanical, and Optical Results of PLA and CuCM/PLA Composites

Sample	MFR (g/10 min)	Transmittance (%)	Haze (%)	Impact strength (kJ/m^2)	Tensile strength (MPa)	Stress at break (MPa)	Elongation at break (%)
PLA	5.82	93.4	1.8	2.67	59.5	45.3	13.6
CuCM0.1%/PLA	8.09	88.9	4.3	2.41	58.2	45.0	8.2
CuCM0.5%/PLA	6.66	74.7	15.3	2.61	50.0	40.0	10.0
CuCM1%/PLA	6.16	64.8	25.4	2.58	51.6	41.7	6.5
CuCM2%/PLA	7.87	42.2	46.3	2.39	43.3	39.9	4.7
CuCM3%/PLA	7.83	21.6	55.0	2.31	37.0	37.0	2.2

result from the chemical structure of this polymer.[33,34] The properties of PLA decided about using PLA for production of CuCMs and detailed analysis of these components.

The objective of the current research was to determine the influence of the CuCMs on selected physical, mechanical and functional properties of PLA. It was the authors' intention to open a new field of application for PLA as a basis for the manufacturing of microbial composites. The research will be continued in the future.

Melt Flow Rate (MFR)

The MFR of the polylactide composites did not significantly change with the rising CuCM content. This quantity was comprised in the range of ca. 5.82–8.09 g/10 min., which does not have much impact on practical applications. The resulting MFR values indicate the possibility of using the materials in processes of injection moulding or extrusion of flat film. A slight increase in MFR may be due to a partial degradation of PLA after the addition of CuCM. The introduction of different amounts of CuCM fillers into the PLA matrix, which cannot be plasticized, may cause an increase of the shearing forces in the plasticizing system, and therefore, the degradation of the polymer. Slight changes of the MFR value may also be caused by the catalytic activity of CuCM, leading to the formation of oligomeric and low-molecular mass products as derivatives of PLA.

Mechanical Properties

The mechanical properties of films of CuCM/PLA composites are shown in Table III. It is shown that the neat PLA has a tensile strength of 59.5 MPa and stress at break of 45.3 MPa. The tensile strength and stress at break were comparable for PLA composites with 0.1 wt % filler loading and pure PLA. At a higher filler loading (3 wt %), the tensile strength and stress at break were decreased to 37% (tensile strength) and to 37% (stress at break), respectively. The worsening strength properties may result from a partial degradation of PLA, which was confirmed by MFR values. Another reason for the tensile strength and the stress at break fall may be insufficient adhesion of both materials, i.e., PLA and CuCM in interface. In spite of worse strength properties of tested composites, the final strength values are high enough for a wide application of new materials.

Much more dramatic changes were observed for the measured elongation at break. The percentage (%) elongation at break of the composites decreased spectacularly upon increasing CuCM content. The parameter decreased by 83.8 from 13.6 to 2.2%. Such situation is often observed in composites with fillers of this kind. The introduction of the pulverized fillers into the polymer matrix like $CaCO_3$ stiffens the material, and macromolecules have a limited possibility for their orientation. Little distortion of the material may be advantageous in some applications, e.g., connected with production of stiff packagings after thermoforming procedure.

Impact Strength

The impact strength of the studied polylactide composites did not significantly change with the rising CuCM content. This quantity was comprised in the range of ca. 2.3–2.7 kJ/m^2, which is not important for practical applications. These values pointed out that the samples were brittle to a great extent. The pure PLA could also be considered as brittle since its impact strength (2.6 kJ/m^2) was contained in the range mentioned above.

Haze and Transmittance

Table III shows the value of transmittance of the polymeric films under investigation, incorporating various amount of CuCMs. The transmittance and haze studies revealed that the addition of the carbon component has an influence on the optical appearance of the films: a decrease of transmittance and an increase of haze. The highest transmittance (88.9%) was noticed for a sample of 0.1 wt % CuCM content. Transmittance decreases significantly upon the increase in the content of CuCMs (up to 3 wt %). The obtained results may indicate two effects. First, the decrease of transmittance and an increase of haze may result from a greater ability of macromolecules of PLA to crystallize upon of the CuCM additive. This may indicate that CuCM is a nucleating agent forming nuclei for PLA crystallization. Secondly, when using the CuCM particles, the dispersed phase in the polymer matrix creates an important barrier for transmitting light. However, such reduced transparency is not always a barrier for practical applications, since not all packaging materials need to be transparent. The nontransparent packagings are very important in such applications like: (a) in medicine for packing medicinal compounds susceptible to light, (b) in food industry for packing food products of low resistance to decay, and (c) in agriculture and gardening for manufacturing packagings protecting rooting system of plants from harmful microorganisms.

Antibacterial Activity of Films on *E. coli* and *S. aureus*

The antimicrobial properties of composite PLA films (incorporating the already-tested carbons) against *E. coli* and *S. aureus*, led to similar satisfactory features, since the reduction of $\log_{10}$ reduction often exceeded 2. For example, PLA films containing

3 wt % of active substance (CA-ACu0.05 sample) demonstrated high $\log_{10}$ reduction values of 2.17 and 2.66 for the strains of *E. coli* and *S. aureus*, respectively. Other PLA films containing a less active agent showed a less spectacular activity: $\log_{10}$ reduction ranged from 0.58 to 0.73. Thus, the materials can be considered as neutral in the presence of tested strains.

CONCLUSIONS

The proposed method of fabrication makes it possible to obtain new carbons of antimicrobial properties due to the presence of highly dispersed CuO and/or Cu_2O. The carbons can be successfully applied for the fabrication of new composite PLA films showing high and similar antibacterial properties. The modified films consist of biodegradable PLA (over 97 wt %) and copper-carbon materials (up to 3 wt %). Despite the low content of carbon material, several composite PLA films exhibited excellent microbial activity against selected gram-positive (*S. aureus*) and gram-negative bacteria (*E. coli*). The PLA films retained high mechanical strength due to the compatibility of carbon material to PLA. These composites show a high and satisfactory tensile strength, and stress at break at all compositions (only a minor decrease was noticed). These materials are suitable for miscellaneous and wide functional applications, thanks to the high biological activity of the films with copper carbon materials, their durability and resistance.

ACKNOWLEDGMENTS

This work was partly supported by the Scholarship Program of the Marshall of the Kuyavian-Pomeranian Voivodeship "Step into the future scholarships for PhD students fifth edition".

REFERENCES

1. Le Pape, H.; Solano-Serena, F.; Contini, P.; Devillers, C.; Maftah, A.; Leprat, P. *Carbon* **2002**, *40*, 2947.
2. Le Pape, H.; Solano-Serena, F.; Contini, P.; Devillers, C.; Maftah, A.; Leprat, P. *J. Inorg. Biochem.* **2004**, *98*, 1054.
3. Ortiz-Ibarra, H.; Casillas, N.; Soto, V.; Barcena-Soto, M.; Torres-Vitela, R.; de la Cruz, W.; Gómez-Salazar, S. *J. Colloid Interface Sci.* **2007**, *314*, 562.
4. Park, H. J.; Kim, J. Y.; Kim, J.; Lee, J. H.; Hahn, J. S.; Gu, M. B.; Yoon, J. *Water Res.* **2009**, *43*, 1027.
5. Khare, P.; Sharma, A.; Verma, N. *J. Colloid Interface Sci.* **2014**, *418*, 216.
6. Montag, J.; Schreiber, L.; Schönherr, J. *J. Phytopathol.* **2006**, *154*, 474.
7. Brzeziński, S.; Malinowska, G.; Kowalczyk, D.; Kaleta, A.; Borak, B.; Jasiorski, M.; Dąbek, K.; Baszczuk, A.; Tracz, A. *Fibres Textiles Eastern Eur.* **2012**, *1*, 70.
8. Nicoletti, G.; Domalewska, E.; Borland, R. *Mycol. Res.* **1999**, *103*, 1073.
9. Stavitskaya, S. S.; Tomashevskaya, A. N.; Goba, V. E.; Kartel, N. T. *Russ. J. Appl. Chem.* **2003**, *76*, 44.
10. Lee, Y. J.; Kim, S.; Park, S. H.; Park, H.; Huh, Y. D. *Mater. Lett.* **2011**, *65*, 818.
11. Jia, B.; Mei, Y.; Cheng, L.; Zhou, J.; Zhang, L. *ACS Appl. Mater. Interfaces* **2012**, *4*, 2897.
12. Palza, H.; Gutierrez, S.; Delgado, K.; Salazar, O.; Fuenzalida, V.; Avila, J. I.; Figueroa, G.; Quijada, R. *Macromol. Rapid Commun.* **2010**, *31*, 563.
13. Biniak, S.; Świątkowski, A.; Pakuła, M. In Chemistry and Physics of Carbon; Radovic, L. R., Ed.; Dekker: New York, **2001**.
14. Świątkowski, A.; Pakuła, M.; Biniak, S.; Walczyk, M. *Carbon* **2004**, *42*, 3057.
15. Pakuła, M.; Świątkowski, A.; Walczyk, M.; Biniak, S. *Colloids Surf. A: Physicochem. Eng. Aspects* **2005**, *260*, 145.
16. Walczyk, M.; Świątkowski, A.; Pakuła, M.; Biniak, S. *J. Appl. Electrochem.* **2005**, *35*, 123.
17. Pakula, M.; Walczyk, M.; Biniak, S.; Swiatkowski, A. *Chemosphere* **2007**, *69*, 209.
18. Biniak, S.; Pakuła, M.; Świątkowski, A.; Walczyk, M. In Carbon Materials—Theory and Practice; Terzyk, A. P.; Gauden, P. A.; Kowalczyk, P., Eds.; Research Signpost: Kerala, **2008**, Chap. 3.
19. Kucinska, A.; Golembiewski, R.; Lukaszewicz, J. P. *Sci. Adv. Mater* **2014**, *6*, 290.
20. Kucinska, A.; Cyganiuk, A.; Lukaszewicz, J. P. *Carbon* **2012**, *50*, 3098.
21. Kucińska, A.; Łukaszewicz, J. P. Patent application P.396955 (**2011**).
22. Kucińska, A.; Łukaszewicz, J. P. *Inżynieria I Ochrona Środowiska* **2013**, *16*, 191.
23. Ilnicka, A.; Gauden, P. A.; Terzyk, A. P.; Lukaszewicz, J. P. *J. Nanosci. Nanotechnol.* **2015**, *15*, 1.
24. Byeon, J. H.; Yoon, K. Y.; Park, J. H.; Hwang, J. *Carbon* **2007**, *45*, 2313.
25. Ruparelia, J. P.; Chatterjee, A. K.; Duttagupta, S. P.; Mukherji, S. *Acta Biomater.* **2008**, *4*, 707.
26. Liou, R. M.; Chen, S. H. *J. Hazard. Mater.* **2009**, *172*, 498.
27. Biniak, S.; Pakuła, M.; Szymański, G. S.; Świątkowski, A. *Langmuir* **1999**, *15*, 6117.
28. Stoimenov, P. K.; Klinger, R. L.; Marchin, G. L.; Klabunde, K. J. *Langmuir* **2002**, *18*, 6679.
29. Palmer, D. A. *J. Sol. Chem.* **2011**, *40*, 1067.
30. Azimirad, R.; Safa, S. *Synth. React. Inorg. Metal-Org. Nano-Metal Chem.* **2014**, *44*, 798.
31. Pham, A. N.; Xing, G.; Miller, C. J.; Waite, T. D. *J. Catal.* **2013**, *301*, 54.
32. Baes, C. F.; Mesmer, R. E. The Hydrolysis of Cations; Wiley: New York, **1976**.
33. Malinowski, R.; Janczak, K.; Rytlewski, P.; Raszkowska-Kaczor, A.; Moraczewski, K.; Żuk, T. *Compos. B: Eng.* **2015**, *76*, 13.
34. Garlotta, D. *J. Polym. Environ.* **2001**, *9*, 63.